




Virulence as a Side Effect of Interspecies Interaction in *Vibrio* Coral Pathogens

 Esther Rubio-Portillo,^{a,b} Ana B. Martin-Cuadrado,^a Andrés M. Caraballo-Rodríguez,^c Forest Rohwer,^{b,d} Pieter C. Dorrestein,^c Josefa Antón^a

^aDepartment of Physiology, Genetics and Microbiology, University of Alicante, Alicante, Spain

^bDepartment of Biology, San Diego State University, San Diego, California, USA

^cSkaggs School of Pharmacy and Pharmaceutical Sciences, University of California, San Diego, La Jolla, California, USA

^dViral Information Institute, San Diego State University, San Diego, California, USA

ABSTRACT The increase in prevalence and severity of coral disease outbreaks produced by *Vibrio* pathogens, and related to global warming, has seriously impacted reef-building corals throughout the oceans. The coral *Oculina patagonica* has been used as a model system to study coral bleaching produced by *Vibrio* infection. Previous data demonstrated that when two coral pathogens (*Vibrio coralliilyticus* and *Vibrio mediterranei*) simultaneously infected the coral *O. patagonica*, their pathogenicity was greater than when each bacterium was infected separately. Here, to understand the mechanisms underlying this synergistic effect, transcriptomic analyses of monocultures and cocultures as well as experimental infection experiments were performed. Our results revealed that the interaction between the two vibrios under culture conditions overexpressed virulence factor genes (e.g., those encoding siderophores, the type VI secretion system, and toxins, among others). Moreover, under these conditions, vibrios were also more likely to form biofilms or become motile through induction of lateral flagella. All these changes that occur as a physiological response to the presence of a competing species could favor the colonization of the host when they are present in a mixed population. Additionally, during coral experimental infections, we showed that exposure of corals to molecules released during *V. coralliilyticus* and *V. mediterranei* coculture induced changes in the coral microbiome that favored damage to coral tissue and increased the production of lysoplatelet activating factor. Therefore, we propose that competition sensing, defined as the physiological response to detection of harm or to the presence of a competing *Vibrio* species, enhances the ability of *Vibrio* coral pathogens to invade their host and cause tissue necrosis.

IMPORTANCE *Vibrio coralliilyticus* and *Vibrio mediterranei* are important coral pathogens capable of inducing serious coral damage, which increases severely when they infect the host simultaneously. This has consequences related to the dispersion of these pathogens among different locations that could enhance deleterious effects on coral reefs. However, the mechanisms underlying this synergistic interaction are unknown. The work described here provides a new perspective on the complex interactions among these two *Vibrio* coral pathogens, suggesting that coral infection could be a collateral effect of interspecific competition. Major implications of this work are that (i) *Vibrio* virulence mechanisms are activated in the absence of the host as a response to interspecific competition and (ii) release of molecules by *Vibrio* coral pathogens produces changes in the coral microbiome that favor the pathogenic potential of the entire *Vibrio* community. Thus, our results highlight that social cues and competition sensing are crucial determinants of development of coral diseases.

Citation Rubio-Portillo E, Martin-Cuadrado AB, Caraballo-Rodríguez AM, Rohwer F, Dorrestein PC, Antón J. 2020. Virulence as a side effect of interspecies interaction in *Vibrio* coral pathogens. *mBio* 11:e00201-20. <https://doi.org/10.1128/mBio.00201-20>.

Editor Nicole Dubilier, Max Planck Institute for Marine Microbiology

Copyright © 2020 Rubio-Portillo et al. This is an open-access article distributed under the terms of the [Creative Commons Attribution 4.0 International license](https://creativecommons.org/licenses/by/4.0/).

Address correspondence to Esther Rubio-Portillo, esther.portillo@ua.es.

Received 5 February 2020

Accepted 19 June 2020

Published 21 July 2020

KEYWORDS *Vibrio*, virulence, competition, coral diseases, transcriptome

The coral holobiont is a very rich consortium whose components interact in complex ways (1). Within natural environments, many taxa coexist in close proximity, and bacteria have evolved to sense and adapt to cues from neighboring species to enable them to communicate, cooperate, or compete (2). These species interactions define the pathogenic potential of the entire community (3, 4). Currently, it is well known that many coral diseases are caused by a diverse polymicrobial consortium (5–7). Two species in particular, *Vibrio mediterranei* (= *Vibrio shilonii*) (8) and *Vibrio coralliilyticus*, have caused coral deaths worldwide (9–15). Potential virulence factors have been identified by sequencing the genomes of these two *Vibrio* species (16–18) (and each of them has been shown to be virulent in laboratory coral infection assays [9, 10, 19, 20]). Although most infection experiments have studied these species separately, we recently demonstrated increased virulence and higher coral tissue damage under conditions in which *V. coralliilyticus* and *V. mediterranei* were inoculated simultaneously in *Oculina patagonica*, suggesting that the presence of both species resulted in a synergistic effect on pathogenic behavior (15). It was previously suggested that bacterial intraspecific competition can increase virulence (21), but that study did not present details about how virulence factors could be regulated by intraspecific competition. Thus, investigations of whether *V. coralliilyticus* and *V. mediterranei* interact synergistically may improve our understanding of coral diseases and facilitate the development of effective disease control strategies. Within this framework, the main goal of this study was to elucidate the mechanisms involved in pathogenic synergy and virulence factor regulation in response to the presence of another pathogen. Transcriptional responses were evaluated at two temperatures under monoculture and coculture conditions. These experiments showed that these two bacteria increased production of multiple virulence factors during coculture (in the absence of corals) in a temperature-dependent manner specific to each species. These findings highlight that competition sensing, defined as a physiological response to detection of harm or to the presence of a competing *Vibrio* species, increased the pathogenic potential in these two coral pathogens, which could favor host invasion. Additionally, we showed that metabolites released by these two coral pathogens influenced the coral microbial community, favoring the growth of other potential pathogens and subsequent coral tissue necrosis.

RESULTS AND DISCUSSION

Growth and cocultivation. The growth of the two vibrios was monitored in monoculture and coculture by DAPI (4',6-diamidino-2-phenylindole) and FISH (fluorescence *in situ* hybridization) counts, respectively (see Fig. S1 in the supplemental material). Growth rates were similar for monocultures of the two species, although *V. mediterranei* grew slightly faster than *V. coralliilyticus* at 20°C whereas *V. coralliilyticus* grew faster than *V. mediterranei* at 28°C. Although both species grew slower in coculture, the growth of *V. mediterranei* was less influenced by cocultivation at 20°C and *V. coralliilyticus* was less affected at 28°C. Therefore, growth data suggest that *V. mediterranei* is more adapted to 20°C and *V. coralliilyticus* to 28°C.

Transcriptomic analysis under coculture conditions. During exponential growth of each culture, RNA was extracted and sequenced for transcriptome analysis by comparison of the genomes of *V. coralliilyticus* and *V. mediterranei*, which were sequenced and analyzed as described above. The main features of these genomes are shown in Table S2 in the supplemental material. Transcriptome sequencing (RNA-seq) data from replicates from the same condition were highly reproducible, showing Pearson coefficient values between 0.977 and 0.981. Between 1.29×10^6 and 9.08×10^6 forward reads were obtained for each of the eight samples, and the total number was reduced to between 4.5×10^5 and 3.84×10^6 mRNA reads after excluding reads mapping to rRNA genes (Table S3). The percentage of expressed open reading frames (ORFs) depended on the growth conditions, with significantly fewer ORFs

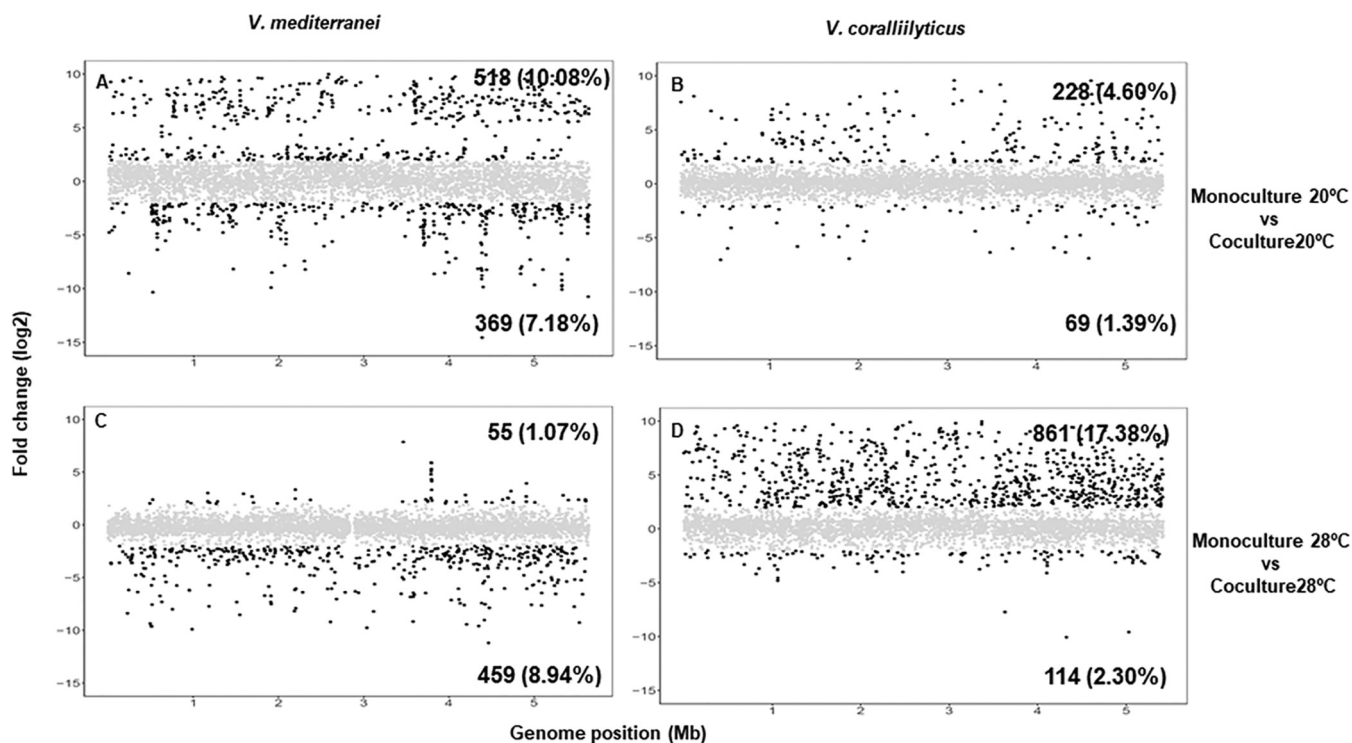


FIG 1 Fold changes across the genomes of *V. mediterranei* and *V. coralliilyticus*. The plots show comparisons between coculture and monoculture conditions at 20°C (A and B) and 28°C (C and D). In each plot, the genes that have a fold change (\log_2) of greater than 2 or less than -2 in the genomes of *V. mediterranei* (A and C) and *V. coralliilyticus* (B and D) are colored in black. Genes represented in gray are those with fold change values between -2 and 2 . The number of genes upregulated (upper right corner in each plot) or downregulated (bottom right corner in each plot) and the percentage of total genes affected are shown in bold.

expressed under coculture conditions at 20°C and 28°C for *V. coralliilyticus* and *V. mediterranei*, respectively (Table S4), which was consistent with the growth rate data shown before. A comparison of gene expression levels clearly showed that, for the two strains, cocultures had significantly more overexpressed genes at 20°C and 28°C for *V. mediterranei* and *V. coralliilyticus*, respectively (Fig. 1). More specifically, for *V. mediterranei* at 20°C, 887 genes were differentially expressed in coculture compared with monoculture (Fig. 1A). Among these, 518 genes were upregulated and most of them were related to environmental adaptation, cell motility, signaling molecules and interactions, drug resistance, virulence, and enzyme synthesis (Fig. S2A). In *V. coralliilyticus*, 975 genes were differentially expressed in coculture compared with monoculture at 28°C and 861 of these were upregulated (Fig. 1D). Most of those genes with known function were classified as metabolic genes, but approximately 20% were related to infection diseases, enzyme synthesis, cellular community, cell motility, and drug resistance (Fig. S2D). In summary, the results showed that a great proportion of the upregulated genes under coculture conditions were related to competition sensing and virulence. Among them, genes of known functional and pathogenic significance were selected and further analyzed as described below.

Virulence-related genes overexpressed in cocultures. (i) The siderophore systems. Genes encoding iron transporters were overexpressed under coculture conditions (Fig. 2). Using antiSMASH (22), we identified aerobactin siderophore biosynthetic clusters in chromosome II from both *Vibrio* spp. In *V. mediterranei*, this cluster included 12 ORFs, which were overexpressed in coculture at 20°C but not at 28°C. Conversely, in *V. coralliilyticus*, this cluster (with 10 ORFs) was highly upregulated under coculture conditions at 28°C (Fig. 3). These differences were not due to different iron concentrations under monoculture and coculture conditions, as chemical analysis indicated that the iron concentrations were similar under both conditions (Fig. S3). It can be con-

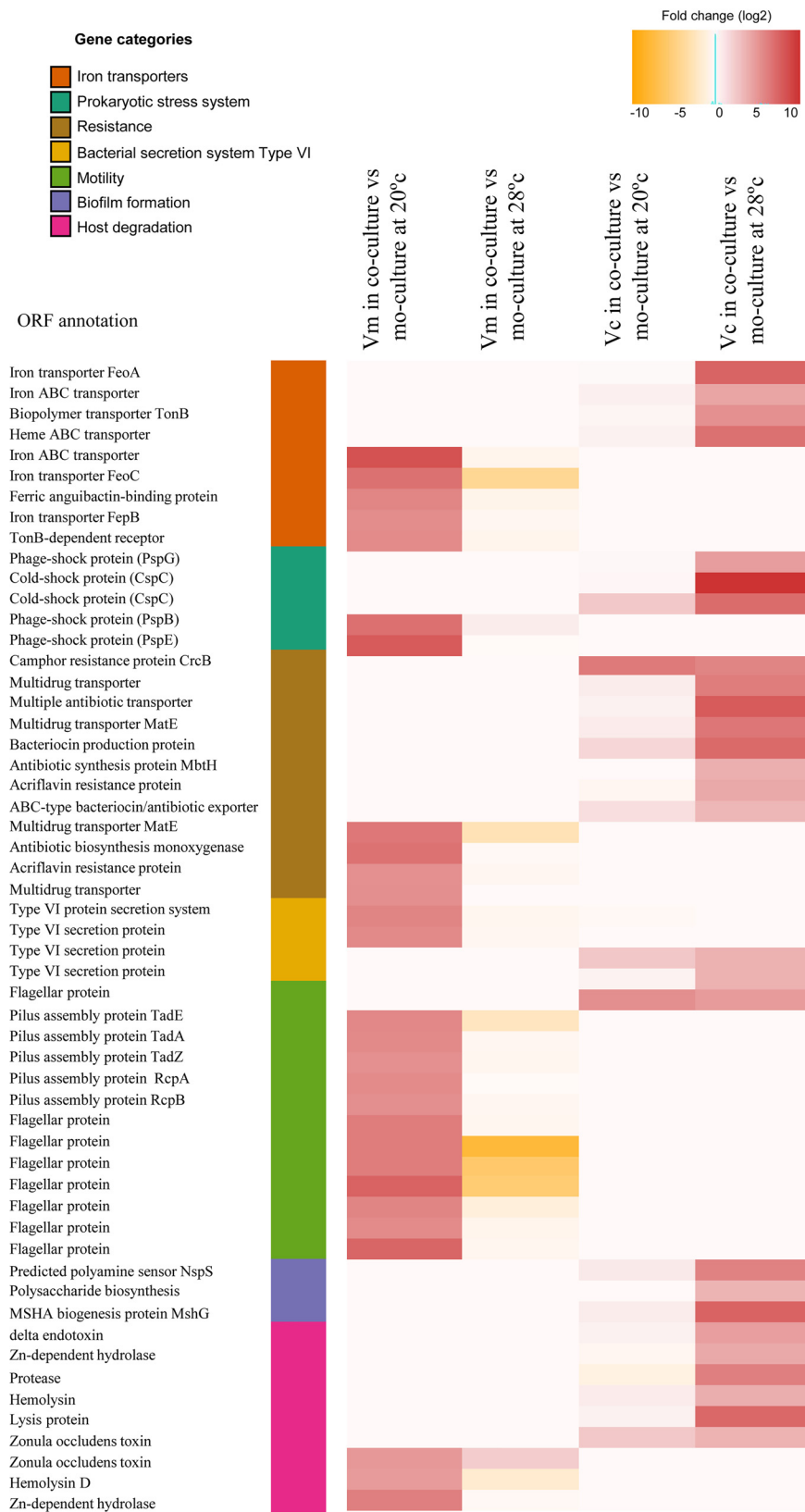


FIG 2 Heat map visualization of *Vibrio mediterranei* (Vm) and *Vibrio coralliilyticus* (Vc) genes that showed more highly differential expression levels under monoculture and coculture conditions. Each row represents a gene (ordered by categories), and each cell represents the fold change detected between the conditions.

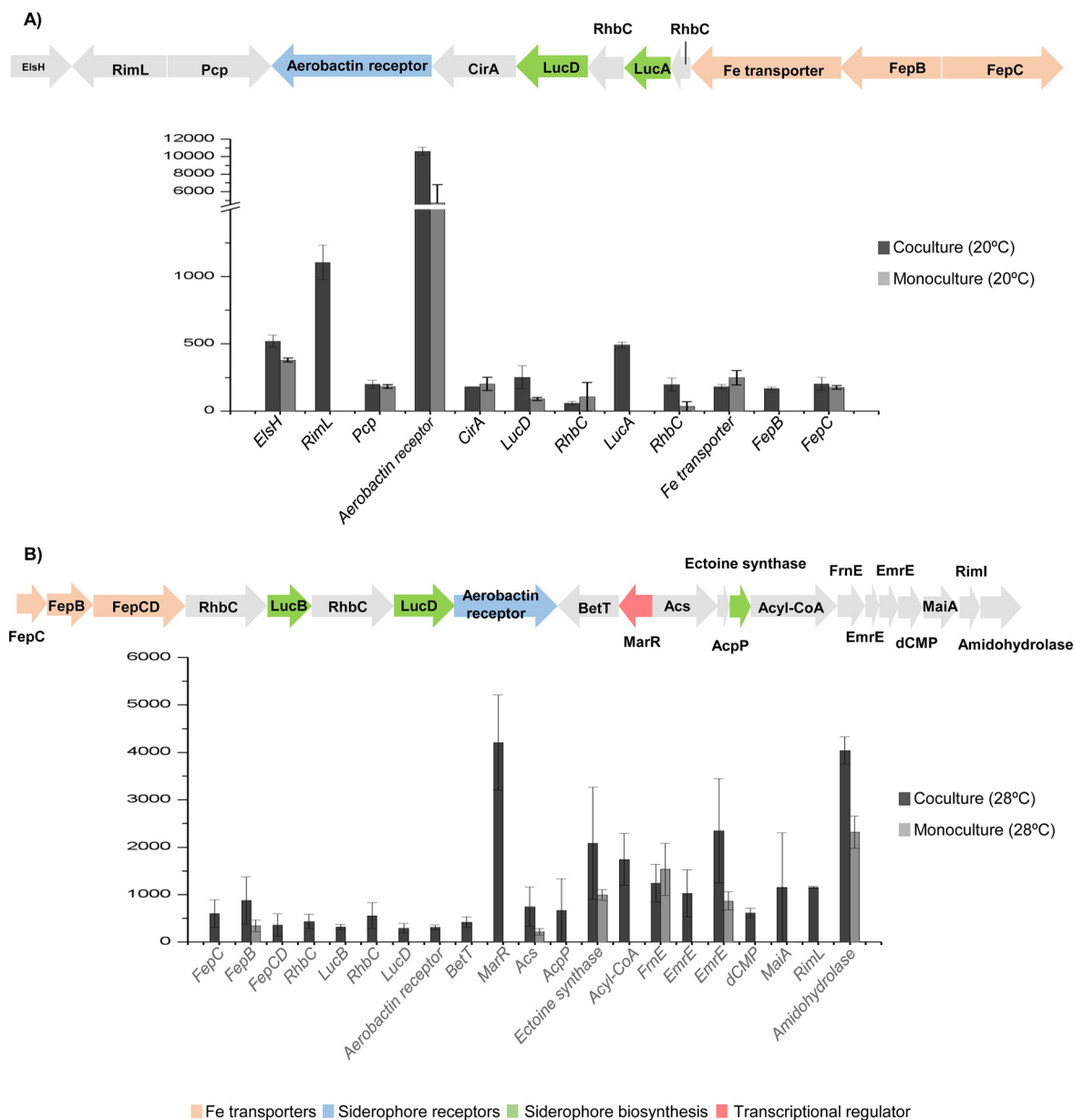


FIG 3 Expression levels of siderophore biosynthesis genes under *Vibrio* coculture conditions. (A) Siderophore biosynthesis cluster of *Vibrio mediterranei* and the reads per kilo base per million reads (RPKM) values of each gene expression measured at 20°C in monoculture and coculture conditions. (B) Siderophore biosynthesis cluster of *Vibrio coralliilyticus* and the reads per kilo base per million reads (RPKM) values of each gene expression measured at 28°C in monoculture and coculture conditions. Acyl-CoA, acyl coenzyme A.

cluded that siderophores may have been produced because of the presence of the other *Vibrio* spp. in the cocultures in a manner similar to that previously detected for an increase of siderophore production as a response to competitors in *Pseudomonas aeruginosa* (23, 24). In addition to iron acquisition, siderophores in pathogenic vibrios are also involved in production of several virulence factors such as toxins (25), biofilm formation (26), and swarming motility (27). Thus, *Vibrio* coral pathogens that produce siderophores in complex microbial communities may have a selective advantage through their ability to obtain iron that is not freely available in the coral host such as has been described previously in other *Vibrio* species (28). This production could also increase *Vibrio* virulence through, for instance, toxin production (see below).

(ii) Type VI secretion systems. Bacteria have a variety of specialized secretion systems that enable cells to respond to the environment through adhesion, pathoge-

nicity, adaptation, and competition (29). The type VI secretion system (T6SS) proteins function as virulence factors against eukaryotic and prokaryotic cells and play an important role during antagonistic interactions with competing microorganisms (30). In *Vibrio cholerae*, the T6SS is a contact-dependent weapon that enables direct killing of other cells by the translocation of proteinaceous toxins into its competitors. Therefore, this system plays an important role during antagonistic interactions with competing microorganisms, promoting *V. cholerae* survival in the aquatic lifestyle and in human hosts (31). In our experiments, genes encoding T6SS-related proteins were clearly upregulated in both *Vibrio* species under coculture conditions (fold change > 4; Fig. 2). *V. mediterranei* genes related to the T6SS were upregulated in cocultures at 20°C, while they were upregulated in *V. coralliilyticus* at 28°C. Therefore, the activation of T6SS as a competition sensing mechanism in *Vibrio* cocultures was able to promote interspecies toxicity and to favor *V. mediterranei* and *V. coralliilyticus* survival against competing microorganisms during coral colonization at 20 and 28°C, respectively.

(iii) Prokaryotic stress systems. Typically, stress responses are initiated to enable cells to adapt to a new environment, such as a change in nutrient availability, species competition, or attack from the host immune system. For this reason, stress responses could be considered a mechanism to detect ecological competition from other cells that are present (32). A common strategy followed by several microbes in this ecological competition is that of developing antibiotic resistance as a response to the threat of toxin attack by other cells (32). In our experiments, genes related to efflux pumps and drug resistance were more highly expressed under coculture conditions than under monoculture conditions (Fig. 2), suggesting that the products of these genes could mediate competition between these species. In addition to antibiotic resistance, we detected upregulation of proteins related to other stress responses in cocultures. *V. mediterranei* overexpressed genes related to phage shock proteins (Psp) at 20°C (Fig. 2), while genes encoding cold shock proteins (Csp) were upregulated in *V. coralliilyticus* at 28°C. The Psp response induces synthesis of essential mechanisms for virulence in many pathogens (33, 34), while Csp-like proteins play an important role in survival during host colonization (35). Consequently, when these two *Vibrio* species cooccur in the coral host, activating stress responses could favor *V. mediterranei* and *V. coralliilyticus* survival during coral colonization at 20 and 28°C, respectively.

(iv) Motility. *Vibrio* species have a dual flagellar system that includes a constitutive polar flagellum required for swimming motility and a lateral flagellar system related to swarming motility that is induced only under certain conditions and is essential for movement in viscous environments (36–38). According to our findings, the lateral flagellar locus in *V. mediterranei* was overexpressed under coculture conditions at 20°C, together with genes that encode the tight adherence pili (Fig. 2), which are essential for adherence, biofilm formation, colonization, and pathogenesis (39). Similarly, several genes involved in biogenesis of the type IV mannose-sensitive hemagglutinin (MSHA) pilus were upregulated in *V. coralliilyticus* under coculture conditions at 28°C (Fig. 2). Overexpression of MSHA genes was previously detected in heat-activated *V. coralliilyticus* transcriptomes (18), and these genes were also previously found to be involved in biofilm formation (40). Therefore, the interaction between *V. mediterranei* and *V. coralliilyticus* coral pathogens may induce changes in motility and biofilm formation that could favor coral colonization.

(v) Production of lytic enzymes and toxins. Pathogenic bacteria produce different substances that are directly or indirectly toxic to host cells; for example, lytic enzymes that cause damage to host tissues are known to play a central role in pathogenesis (41). Our results show that both species produced hemolysins and Zn-dependent metalloproteases in cocultures and that *V. coralliilyticus* also produced proteases (Fig. 2). It has been reported previously that Zn metalloproteases produced by *V. mediterranei* and *V. coralliilyticus* cause photosynthetic inhibition of the coral dinoflagellate endosymbiont *Symbiodinium* (87). In addition to lytic enzymes, these two *Vibrio* species in coculture also overexpressed the gene that encodes the zonula occludens toxin (Zot) (Fig. 2). In *V. cholerae*, this phage-encoded toxin increases the permeability of the human intes-

tinal epithelium through reorganization of the cytoskeleton filaments by actin polymerization (42) and may have the same effect in the coral epithelial cell barrier (Rubio-Portillo et al., unpublished results).

(vi) Noncoding RNAs (ncRNAs) as virulence regulators. ncRNAs are small RNA transcripts (typically 50 to 250 nucleotides) that are not translated into proteins but instead play important roles as posttranscriptional regulators involved in diverse bacterial processes that include stress responses and pathogenicity (43, 44). Among the transcript families identified here, CsrB/RsmB and PrrB/RsmZ RNA had the highest overexpression in both species (Fig. S4). CsrB/RsmB ncRNAs participate in several global regulatory circuits such as cell motility, quorum sensing, and pathogenesis (45–47). RNAs within the PrrB/RsmZ family are structurally similar to CsrB/RsmB and might have similar roles (48). Overall, our results suggest that CsrB and (to a lesser extent) PrrB may be master regulators of the synergistic pathogenicity when the two vibrios grow together. This fits with the observed increased transcription of genes involved in toxin production and expression of flagellar genes, together with the observed rise in levels of cell density (quorum)-sensing signals or their associated pathogenic machinery. Because ncRNAs are not translated and thus are immediately available, they might rapidly modulate a wide range of cellular responses, which would allow *Vibrio* spp. to sense and rapidly respond to putative competitors or environmental stimuli.

In summary, transcriptional data show that *V. mediterranei* and *V. coralliilyticus* were able to detect competitor cells and respond to ecological competition by producing siderophores for survival in the coral host, producing virulence factors (T6SS, toxins) against the host and associated microorganisms and expressing swarming motility and forming biofilms for host adherence. The activation of these mechanisms as a consequence of interspecific competition might favor *Vibrio* pathogenicity. Interestingly, the transcriptional responses to the interactions at 20 and 28°C were different for each species; whereas *V. mediterranei* displayed higher pathogenic potential at 20°C, *V. coralliilyticus* seemed to be more virulent at 28°C. These results agree with our previous results that showed that *V. mediterranei* and *V. coralliilyticus* induced more signs of disease in corals at lower temperature in cocultures than in the natural environment (15). Taken together, these results highlight the harmful potential of coral pathogens when they coexist in the same host. This raises concerns about the possible deleterious effects of the dispersal of pathogens among different locations and their consequences for coral health worldwide.

O. patagonica infection experiments. Considering that our transcriptomic results highlighted the importance of interactions for the pathogenic potential of *Vibrio* and that corals species harbor a natural *Vibrio* community, we also attempted to determine how molecules released by *Vibrio* pathogens would affect *Vibrio* coral assemblages and coral health. With this purpose, laboratory infection experiments were conducted at two different temperatures (20 and 28°C). In these experiments, to distinguish between the effects of direct contact between *Vibrio* cells and coral and the effects of molecules released by *Vibrio* cells, corals were inoculated with the *Vibrio* coculture in either of two ways: cells were either free to interact with the coral or were contained inside a dialysis membrane. Thus, together with corresponding (uninfected) controls, three different treatments were set for each temperature: an infected tank where cells were free, a *Vibrio* coculture dialyzed tank, and a *Vibrio* monoculture dialyzed tank (Fig. 4). The health of the coral fragments used in the experiments was assessed by measurements of concentrations of chlorophyll *a* (Chl *a*) in their tissues. *Vibrio* cells in coral tissues were quantified by diluting and plating crushed coral tissue and counting the resulting *Vibrio* colonies.

Effects on coral health status. Results showed that the chlorophyll *a* concentrations decreased significantly with temperature in all treatments (analysis of variance [ANOVA] $P < 0.001$) (Fig. 5A) and that increases in *Vibrio* abundances were detected concurrently (ANOVA $P < 0.001$) (Fig. 5B). Corals infected with *Vibrio* and corals in the presence of *Vibrio* cocultures inside dialysis membranes showed a decrease in chloro-

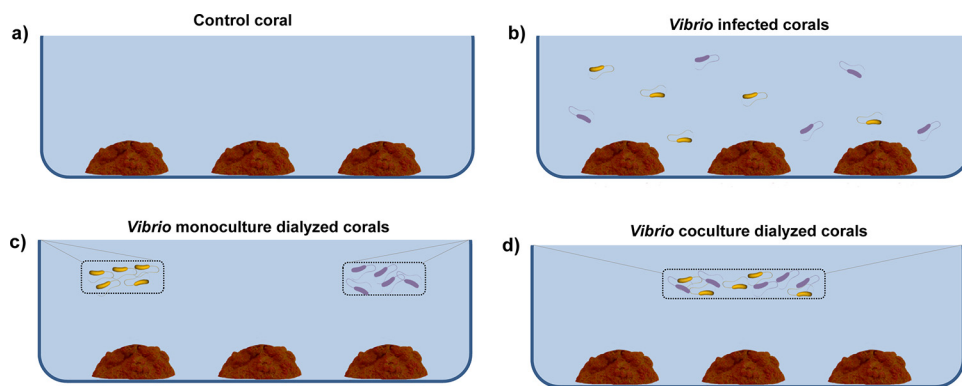


FIG 4 Coral infection experiment working scheme. (a) Control coral tank. (b) Tank with *Vibrio*-infected corals. (c) Tank with *Vibrio* monoculture dialyzed corals. (d) Tank with *Vibrio* coculture dialyzed corals.

phyll *a* concentrations in their tissues compared to controls, independently of seawater (SW) temperature (Fig. 5A). Therefore, vibrios inside the membranes were likely producing molecules that affected the coral *Vibrio* community and coral health status. Nevertheless, the concentration of *Vibrio* in their tissues was statistically significant only at 28°C (Fig. 5B).

Metabolome analysis showed a high abundance of platelet activating factors (PAF), such as Lyso-PAF-C:16, in *O. patagonica* tissues exposed to vibrios (Fig. 6A and B). Activation of Lyso-PAFs has been seen previously in terrestrial invertebrates in response to tissue damage (49), as well as in corals (50–52). Lyso-PAFs seem to be an important element of the immune responses of basal metazoans (51) and have antimicrobial properties (53). The levels of this class of phospholipids were measured for all coral samples, and their relative abundances were higher in infected corals and corals in the presence of *Vibrios* than in the control corals. Curiously, the abundance of Lyso-PAF-C:16 was higher in coral tissues when *O. patagonica* was exposed to *Vibrio* strains inside dialysis membranes at 20°C (Fig. S5). This fact supports the hypothesis that vibrios produce signaling molecules that induce changes in the coral holobiont and its microbial communities and ultimately affect their health status.

Changes in coral *Vibrio* assemblages induced by exposure to *V. mediterranei* and *V. coralliilyticus*. To assess the abundances of the two *Vibrio* coral pathogens in the coral microbiome, we sequenced the metagenomes of corals used in these exper-

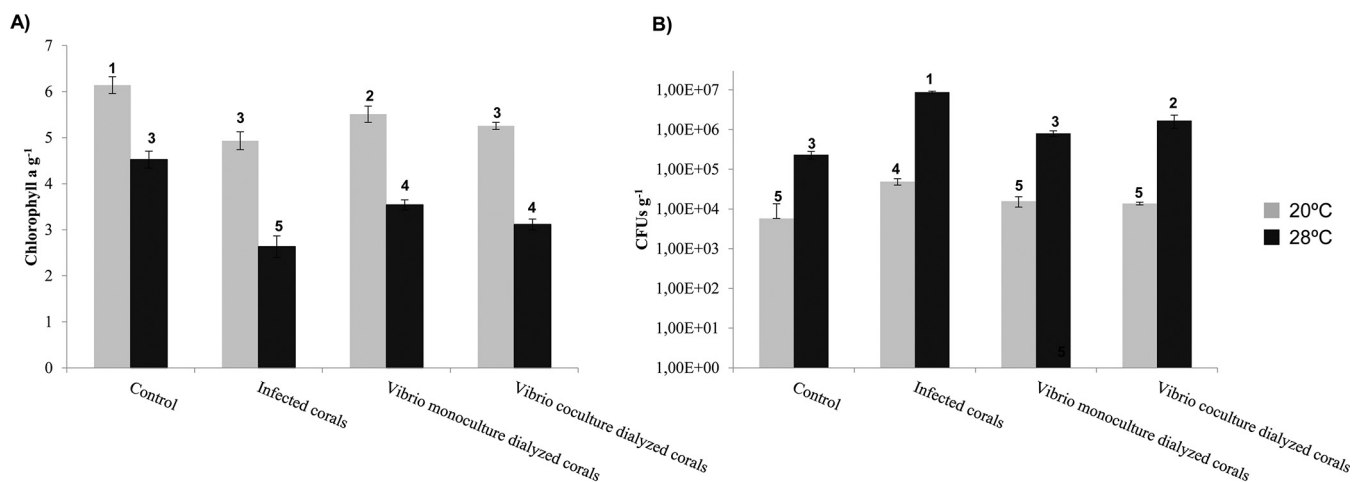


FIG 5 Levels of chlorophyll *a* (A) and concentrations of culturable *Vibrio* species (B) in *O. patagonica* samples after 10 days of experimental infection with the indicated treatment at two different temperatures (20°C and 28°C, shown with gray and black bars, respectively). Groups were defined by *post hoc* Tukey test after ANOVA within each locality and are indicated by numbers at the top of the columns.

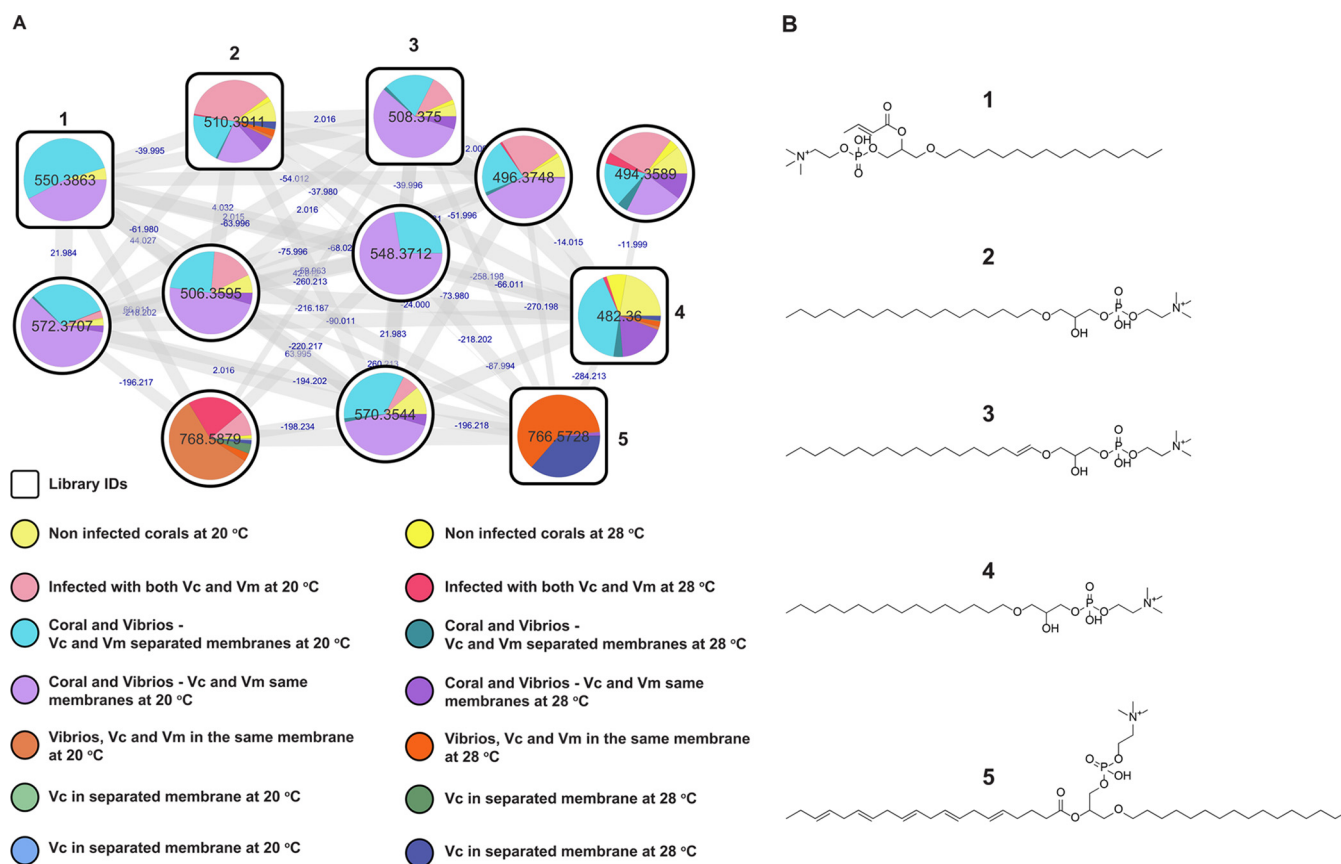


FIG 6 Phospholipid molecular family (platelet activator factor-related molecules, PAFs) from *Oculina patagonica* exposed to *Vibrio coralliilyticus* and *Vibrio mediterranei*. (A) Molecular family showing the relative abundance of detected phospholipids as pie charts. Labeled nodes correspond to the chemical structures in panel B. Each node represents a detected molecular feature. Edges connecting nodes represent spectral similarity, creating subnetworks (molecular families). Edge labels between the connected nodes represent the mass shift between related detected features. Color codes and legends included in the figure correspond to the experimental setup described in the Fig. 4 legend. (B) Chemical structures of putatively identified phospholipids are indicated as follows: 1, feature m/z 550.3863, annotated as 1-O-hexadecyl-2-O-(2E-butenoyl)-sn-glyceryl-3-phosphocholine; 2, feature m/z 510.3911, annotated as 1-octadecyl-sn-glycero-3-phosphocholine (Lyso PC O-18:0); 3, feature m/z 508.3750, annotated as 1-(1Z-octadecenyl)-sn-glycero-3-phosphocholine; 4, feature m/z 482.3600, annotated as 1-O-hexadecyl-sn-glycero-3-phosphocholine (Lyso-PAF); 5, feature m/z 766.5728, annotated as eicosapentaenoyl PAF C-16. Similarity to annotated fragmentation spectra from the GNPS repository and calculated molecular formula based on detected accurate mass were used to identify compounds. These identifications correspond to level 2 for compounds 2 and 4 and level 3 for compounds 1, 3, and 5, as stereochemistry was not established. The levels of identification correspond to suggested annotations according to metabolomics standards (83, 84). IDs, identifiers.

iments and performed fragment recruitment analysis. This analysis indicated that both species were more abundant in corals maintained at 28°C, including the untreated controls (Fig. 7). These results are consistent with our previous findings (54), confirming that these *Vibrio* species form part of the natural coral microbiota and that they increase their abundances in response to elevated seawater temperature. We detected an increase in the levels of these *Vibrio* coral pathogens in coral tissues in directly coinfecting corals compared to control corals, which suggests that these pathogens were actively infecting coral tissues. *V. mediterranei* was more abundant in corals maintained at 20°C, while *V. coralliilyticus* was more abundant at 28°C (Fig. 7). This result, together with the results obtained by transcriptomic analysis and our previous finding that *V. mediterranei* is more virulent at 20°C and *V. coralliilyticus* is more virulent at 28°C (15), suggests that *V. mediterranei* is more highly adapted to low temperatures than *V. coralliilyticus*.

An in-depth analysis of the presence or absence of other *Vibrio* species using fragment recruitment-based abundances in coral metagenomes showed that the abundances of *Vibrio splendidus* and *Vibrio atlanticus*, previously reported to be part of the "constitutive" *O. patagonica* microbiota (15), decreased at 28°C and also in infected corals and corals exposed to *Vibrio* coral pathogens in dialysis at 20°C (Fig. S6). In

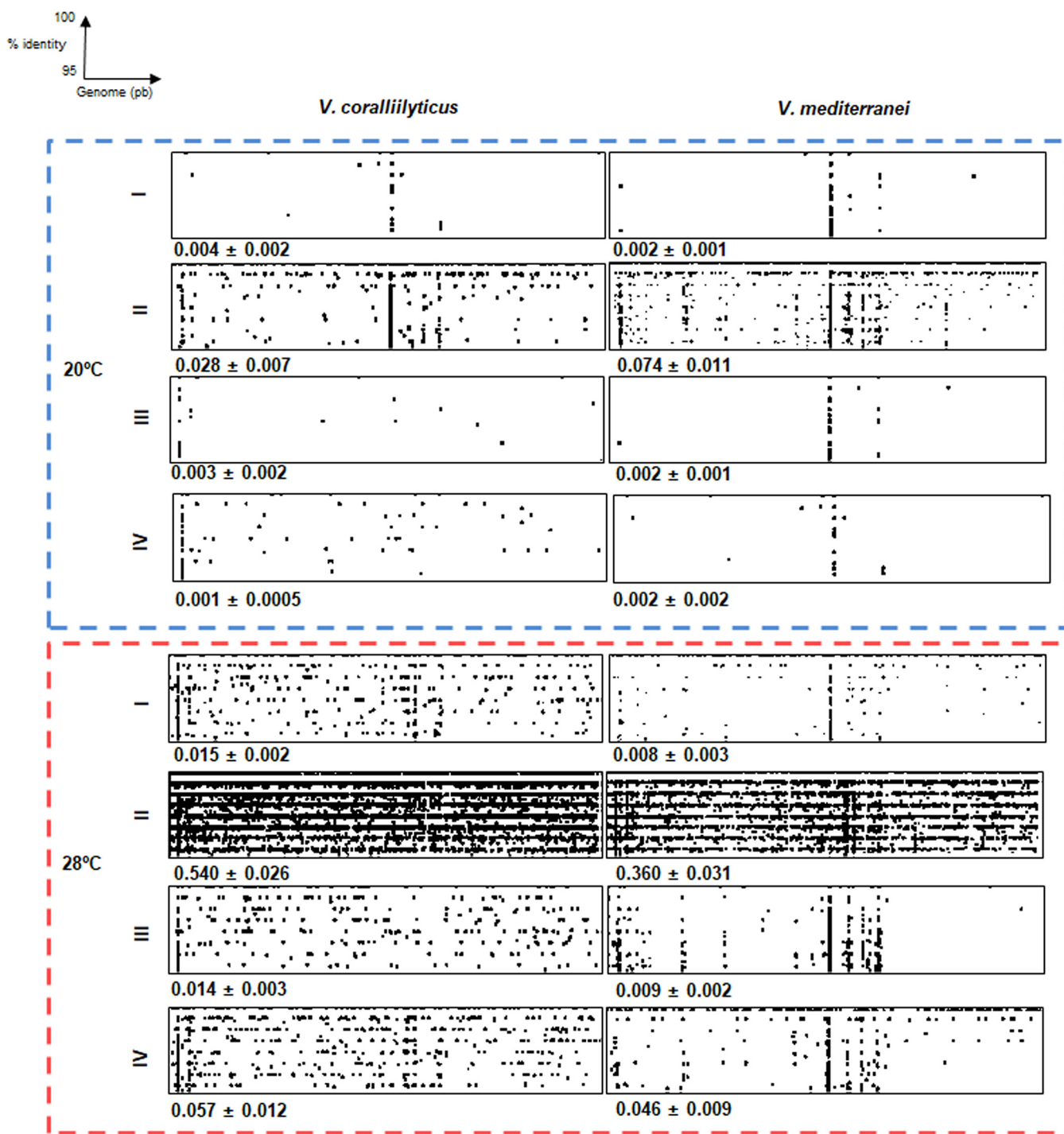


FIG 7 Fragment recruitment plots for metagenome sequence reads of *Vibrio coralliilyticus* and *Vibrio mediterranei* genomes from each coral treatment (treatment I, control corals; II, infected corals; III, corals in the presence of *Vibrio* monocultures; IV, corals in the presence of *Vibrio* coculture). The vertical axis indicates the sequence identity of an alignment between a metagenomic sequence and the reference *Vibrio* genome determined using BLASTn; the levels of identity range from 100% (top) to 95% (bottom). The percentage of reads belonging to each *Vibrio* species is shown in bold in the corner of each plot. Genome (pb), genomes quantified as base pairs.

contrast, the *Vibrio* species that are potential coral pathogens, such as *Vibrio harveyi* or *Vibrio alginolyticus* (55, 56), had increased relative abundances at 28°C and their abundances were even higher in corals that were infected or were maintained in the presence of *V. mediterranei* and *V. coralliilyticus* (Fig. 8). Other example was the well-known human-pathogenic species *Vibrio parahaemolyticus*, which can also cause

and *V. coralliilyticus* cells in cocultures were determined by fluorescence *in situ* hybridization (FISH) with species-specific probes (see below). These probes were also used to check for cross-contamination in monocultures. The growth curves for each condition were used to establish the middle of exponential-growth phase, which was the time point for transcriptome analyses.

(ii) FISH with species-specific probes. *V. mediterranei*-specific and *V. coralliilyticus*-specific probes targeting 16S rRNA were designed with the probe-designing tool of the ARB software package. Based on comparative analysis of all sequences in the Living Tree Project database (LTP project [58]; <http://www.arb-silva.de/projects/living-tree>) and our *Vibrio* genomic sequences, the program selected specific regions to discriminate between the two species. The oligonucleotide probes generated were ViVc-FISH (5'-TCGTTCCCTAAGGTTTCAGACA-3') and ViVm-FISH (5'-CAGTCACCCGAAGGGTCAGTTA-3') for *V. coralliilyticus* and *V. mediterranei*, respectively, and were labeled with Cy-5. Cells were fixed in 4% formaldehyde for 12 h at 4°C and then washed with phosphate-buffered saline (PBS) and kept at 4°C until their analysis. Hybridizations were performed at 46°C for 5 h with hybridization buffer (900 mM NaCl, 20 mM Tris-HCl [pH 8], 0.01% sodium dodecyl sulfate) containing 2 ng of labeled probe/ μ l. The hybridization stringency was adjusted by adding different formamide concentrations (from 10% to 70% [vol/vol] with increments of 10%) to the hybridization buffer (best results were obtained using 40% for ViVc-FISH and 35% for ViVm-FISH). Hybridizations were washed at 48°C for 30 min with washing buffer containing the same components as the hybridization buffer except for the probes and formamide.

(iii) Whole-genome sequencing. Total bacterial DNA was extracted using a DNeasy blood and tissue kit (Qiagen, Valencia, CA) and sequenced using an Illumina MiSeq platform to generate 2×300 -bp reads according to the manufacturer's protocol. Raw reads were cleaned up by trimming the adaptor sequences and low-quality ends (quality score < 30) using Trimmomatic (59). The cleaned reads were *de novo* assembled using the SPAdes Genome Assembler (60). ORF detection was performed with Prodigal (61). Functional annotation was performed by comparing predicted protein sequences through BLAST comparisons against the NCBI-nr database, Pfam (62), COG (63), and TIGRFAM (64) (cutoff E value, 10^{-5}). Ribosomal genes were identified using RNAscan (65). BLAST average nucleotide identity (ANIb) values were calculated based on the whole-genome sequence as described previously by Goris et al. (66). Analysis of the genome completeness was performed using CheckM (67). tRNAscan was used to predict the presence of tRNAs in the genomes as described previously by Lowe and Chan (68). Synteny among the *V. mediterranei* and *V. coralliilyticus* genomes and those of other vibrios was analyzed using the Artemis Comparison Tool (ACT) from Artemis package v.18.0.2 (69). Finally, GC content data were calculated using the "geecee" tool from the emboss package (70).

(iv) RNA extraction and sequencing. Two replicate aliquots from cultures maintained under each set of conditions were centrifuged at $16,000 \times g$ for 15 min, and the resulting cell pellets were preserved at -80°C until RNA was extracted. Total RNA was extracted using an RNeasy minikit (Qiagen) in accordance with the instructions from the manufacturer. Genomic DNA was removed from the extracted RNA by treating the samples with Turbo DNase (Ambion) at 37°C for 45 min. rRNA was partially eliminated with a Ribo-Zero rRNA removal kit (Epicentre), and samples were sequenced using 150-bp paired-end reads on an Illumina NextSeq500 platform.

(v) Analysis of gene expression and detection of differentially expressed genes. Raw reads were cleaned by trimming the adaptor sequences and low-quality ends (quality score < 30) using Prinseq (71). Forward reads were mapped against *Vibrio* genomes using bowtie 2 (72). Once the forward reads from monocultures were mapped to each genome, the reads from cocultures were aligned against a combined reference containing the genomes of *V. mediterranei* and *V. coralliilyticus*. The expression profiles for monocultures were normalized using the number of cells and the ORF length, and these values were provided as RPKM (reads per kilobase per million). Similarly, cocultures were also normalized by the number of cells of each *Vibrio* species. Differentially expressed genes, defined as genes whose expression levels differed more than 2-fold between the two conditions, were identified using DESeq, a variance analysis package that was developed to infer statistically significant differences in gene expression data from high-throughput sequencing (73).

(vi) Analysis of noncoding RNA (ncRNA). We used the cmsearch program as described previously by Cui et al. (74) and the Rfam database (75) to screen for the presence of ncRNAs among the short reads of the transcriptome collections. For this purpose, the remaining ribosomal genes (the 16S, 23S, and 5S rRNA genes) were first removed from the data set using RNAmmer (76). A subset of 10^5 reads was extracted randomly for each of the samples and submitted to the ncRNA screening. For stringency, an E value of 10^{-5} was used as the cutoff.

O. patagonica infection experiments. Fragments (about 5 cm of diameter) of the coral *O. patagonica* were collected in June 2016 (seawater from the Marine Reserve of Tabarca, Spain) and transferred to the laboratory. They were acclimated for 3 days in aquaria (20 liters) and then were randomly assigned to 1 of 8 aquaria (3 liters, 3 pseudoreplicated colonies per aquarium). Afterward, fragments were slowly acclimated to the experimental temperature by increasing the temperature by 0.5°C per day from 18°C (seawater temperature at sampling location) until the final temperature was reached (20 or 28°C). Before inoculation, the corals were maintained at the experimental temperature for 3 days. Water was replaced every 3 days during the 10 days of the infection experiment. In order to study non-contact-dependent effects of *Vibrio* pathogens on coral, a series of infections using dialysis membranes were included in the experiment. These membranes prevented contact between the coral and the *Vibrio* cells but allowed the free dilution of molecules with a molecular weight lower than 100 kDa. One set of four tanks was incubated at 20°C and another set at 28°C . Each set of tanks contained the following: (I) control corals with no *Vibrio* added; (II) corals inoculated with the *Vibrio* coculture; (III) corals with a *Vibrio* coculture growing inside a dialysis membrane; and (IV) corals in the presence of the two *Vibrio* monocultures, each

growing independently inside a dialysis membrane (Fig. 4). Aquaria were inoculated to reach a final bacterial concentration of 10^3 cells/ml of seawater, and the same *Vibrio* concentration was added into the dialysis membranes. At the end of the experiments, coral colonies were gently washed three times with 50 ml of sterile filtered seawater (SFSW) to remove nonassociated bacteria, broken into small pieces, placed in 50-ml tubes, and centrifuged for 3 min at $2,900 \times g$ (Labofuge 400R; Heraeus Instruments) to separate the mucus from the coral tissue and skeleton. After centrifugation, the coral pieces were crushed in SFSW using a mortar and pestle, and the CaCO_3 skeleton was allowed to settle for 15 min before the supernatant (i.e., the crushed tissue) was collected and used for *Vibrio* counts, measurements of chlorophyll *a* (Chl *a*) concentrations, and extractions of DNA and metabolites.

For plate counts of *Vibrio* spp., 10-fold serial dilutions of crushed tissue were prepared in SFSW, plated on thiosulphate citrate bile sucrose (TCBS) agar (Pronadisa, Spain), and incubated at 30°C for 48 h. For Chl *a* measurements, 1 ml of the crushed tissue homogenate was centrifuged at $5,000 \times g$ for 10 min at 4°C (Labofuge 400R; Heraeus Instruments) and the supernatant was discarded, leaving the coral pellet. Pigments were extracted from the coral pellet after an incubation in 10 ml of 90% acetone at 4°C during 24 h in the dark, followed by centrifugation at $13,000 \times g$ for 10 min (Biofuge Pico; Heraeus Instruments). Absorbance readings at 750, 664, 647, and 630 nm were performed as described previously by Jeffrey and Humphrey (77).

(i) Coral metagenomes. Two coral replicates per treatment were used to extract total DNA from the crushed tissue by the use of an UltraClean soil DNA kit (Mo Bio; Carlsbad, CA, USA) following the manufacturer's instructions for maximum yield. Samples were sequenced using 150-bp single-end reads on an Illumina HiSeq 2000 platform. Raw reads were cleaned up by trimming adaptor sequences and low-quality ends (quality score < 30) using Prinseq (71).

Fragment recruitments were performed for different *Vibrio* species to estimate the abundances of these species in the coral samples. We used a database with a total of 9 *Vibrio* genomes (including *V. mediterranei* strain Vic-Oc-097 and *V. coralliilyticus* strain Vic-Oc-068, sequenced in this work, and 7 *Vibrio* spp. previously reported in corals, obtained from GenBank; see Table S1 in the supplemental material). Fragment recruitment analyses were carried out with BLASTN comparisons using version 2.2.31+. Only reads with identities of over 95% and 70% query (read) coverage were considered. When a read hit equally for several vibrios, it was taken into account for all of them using a modification of the BlastTab.best_hit_sorted of Enveomics Toolbox (78). The BlastTab.cast script was used to calculate the sequencing depth of the *Vibrio* genomes and to draw the recruitment plots (enveomics.R library).

(ii) Coral metabolomes and LC-MS/MS data acquisition. One coral replicate per treatment was used to analyze the coral metabolomes. Crushed coral tissue was mixed with 5 ml of cold 70% methanol, incubated for 12 h at 4°C, and stored at -80°C until further analysis. Samples were resuspended in 100% methanol containing 2 μM sulfamethazine as an internal standard, and liquid chromatography-tandem mass spectrometry (LC-MS/MS) analysis was performed in an UltiMate 3000 UPLC (ultraperformance liquid chromatography) system (Thermo Scientific) using a Kinetex 1.7- μm C_{18} 100 Å reversed-phase UHPLC (ultra-high-performance liquid chromatography) column (50 by 2.1 mm) and Maxis Q-TOF (quadrupole-time of flight) mass spectrometer (Bruker Daltonics) equipped with an electrospray ionization (ESI) source. The column was equilibrated with 5% solvent B (LC-MS-grade acetonitrile, 0.1% formic acid) for 1 min, followed by a linear gradient from 5% solvent B to 100% solvent B in 8 min and a hold at 100% solvent B for 3 min. Then, the gradient dilution was changed from 100% solvent B to 5% solvent B in 1 min and was maintained at 5% solvent B for 2 min at a flow rate of 0.5 ml/min throughout the run. MS spectra were acquired in positive-ion mode in the range of 100 to 2,000 *m/z*. Sulfamethazine (2 μM), used as an internal standard, was run after 12 samples (after each row in a 96-well plate). A mixture of 10 mg/ml each of sulfamethazine, sulfamethizole, sulfachloropyridazine, sulfadimethoxine, amitriptyline, and coumarin-314 was run before the analysis and after every 48 injections for quality control. An external calibration with ESI-low-concentration tuning mix (Agilent Technologies) was performed prior to data collection, and the internal calibrant Hexakis (1H,1H,2H-perfluoroethoxy) phosphazene (CAS 186817-57-2) was used throughout the runs. A capillary voltage of 4,500 V, a nebulizer gas pressure (nitrogen) of 2 bar, an ion source temperature of 200°C, a dry gas flow of 9 liters/min source temperature, and spectral rates of 3 Hz for MS1 and 10 Hz for MS2 were used. For acquiring MS/MS fragmentation, the 5 most intense ions per MS1 were selected, the MS/MS active exclusion parameter was enabled and set to 2 and to release after 30 s, and each precursor ion was reconsidered for MS/MS if the current intensity/previous intensity ratio was >2.

Feature finding was performed with open source MZmine software (79, 80) version 2.35 using the following settings: mass detection [MS1 detection at noise level of 10^4 , MS2 detection at noise level of 10^2]; chromatogram building [Min time span: 0.01 min; Min height: 3×10^4 ; *m/z* tolerance: 25 ppm]; deconvolution [Algorithm: Baseline cut-off (Min Peak height: 10^4 ; Peak duration range 0.01–1.0 min; baseline level: 1.0×10^2); *m/z* range for MS2 scan pairing: 0.01 Da; RT range for MS2 scan pairing: 0.3 min]; isotopic peak grouper [*m/z* tolerance: 25 ppm; RT tolerance: 0.2 min; Max charge: 2]; alignment [Join Aligner, *m/z* tolerance: 25 ppm; weight for *m/z*: 75; weight for RT: 25; RT tolerance: 0.2 min]; Gap filling [Peak finder, Intensity tolerance: 1%; *m/z* tolerance: 25 ppm; RT tolerance: 0.2 min; RT correction: checked]; duplicate Peak Filter [Filter mode: new average (create consensus row from duplicates); *m/z* tolerance: 10 ppm; RT tolerance: 0.08 min]; peak filter [Peak area 104–107; Peak duration: 0.00 - 1.00 min]; and peak Row Filtering to export .mgf file to GNPS (Minimum peaks in a row: 2; RT: 1.00–14.00 min). Spectral alignment and molecular networking were performed using the GNPS platform (81, 82). Compounds were identified using GNPS spectral libraries corresponding to level 2 annotations as described previously by Sumner et al. (83). The parameters used for molecular networking analyses can be accessed via the following link: <https://gnps.ucsd.edu/ProteoSAFe/status.jsp?task=2bb970e9782f40eaa50d8b375cfb7444>.

Data availability. *V. mediterranei* and *V. coralliilyticus* genomes were published in GenBank-NCBI under the following BioProject numbers: [PRJNA632837](https://www.ncbi.nlm.nih.gov/bioproject/PRJNA632837) and [PRJNA632838](https://www.ncbi.nlm.nih.gov/bioproject/PRJNA632838). The raw sequences of the transcriptome and metagenome data sets have been deposited in NCBI Sequence Read Archive (SRA) database under BioProject accession number [PRJNA609971](https://www.ncbi.nlm.nih.gov/bioproject/PRJNA609971) and BioProject [PRJNA612159](https://www.ncbi.nlm.nih.gov/bioproject/PRJNA612159), respectively. LC-MS/MS data were deposited in the online repository MassIVE under accession number MSV000083610 and can be accessed as “GNPS - Metabolomes from *O. patagonica* - *V. mediterranei* - *V. coralliilyticus* cocultures” via the following link: <ftp://massive.ucsd.edu/MSV000083610>.

SUPPLEMENTAL MATERIAL

Supplemental material is available online only.

FIG S1, TIF file, 0.1 MB.

FIG S2, TIF file, 2.6 MB.

FIG S3, TIF file, 0.3 MB.

FIG S4, TIF file, 0.9 MB.

FIG S5, TIF file, 3.2 MB.

FIG S6, TIF file, 2.8 MB.

TABLE S1, DOCX file, 0.01 MB.

TABLE S2, DOCX file, 0.01 MB.

TABLE S3, DOCX file, 0.01 MB.

TABLE S4, DOCX file, 0.01 MB.

ACKNOWLEDGMENTS

We acknowledge Francisco García del Portillo for critical reading of the manuscript.

This research was supported in part by the EU-H2020 MetaFluidics project with grant agreement number 685474 (to J.A.) and NSF-PIRE grant number OISE1243541 (to F.R.). E.R.-P. was funded by the postdoctoral program Val+d (GVA) (grant number APOSTD-2016-091). A.M.C.-R. and P.C.D. were supported by the National Sciences Foundation grant IOS-1656481.

E.R.-P. and J.A. conceived and designed the study. E.R.-P. and A.B.M.-C. analyzed the transcriptomic data. A.B.M.-C. and P.C.D. performed the coral metabolome analysis. F.R. contributed with a *Vibrio* transcriptomic and coral metagenomic study. E.R.-P. wrote the manuscript, and all of us contributed substantially with discussion of data and manuscript revisions.

We declare no conflict of interest.

REFERENCES

- Knowlton N, Rohwer F. 2003. Multispecies microbial mutualisms on coral reefs: the host as a habitat. *Am Nat* 162(4 Suppl):S51–S62. <https://doi.org/10.1086/378684>.
- Hibbing ME, Fuqua C, Parsek MR, Peterson SB. 2010. Bacterial competition: surviving and thriving in the microbial jungle. *Nat Rev Microbiol* 8:15–25. <https://doi.org/10.1038/nrmicro2259>.
- Hajishengallis G, Lamont RJ. 2016. Dancing with the stars: how choreographed bacterial interactions dictate nososymbiocity and give rise to keystone pathogens, accessory pathogens, and pathobionts. *Trends Microbiol* 24:477–489. <https://doi.org/10.1016/j.tim.2016.02.010>.
- Stacy A, Everett J, Jorth P, Trivedi U, Rumbaugh KP, Whiteley M. 2014. Bacterial fight-and-flight responses enhance virulence in a polymicrobial infection. *Proc Natl Acad Sci U S A* 111:7819–7824. <https://doi.org/10.1073/pnas.1400586111>.
- Roder C, Arif C, Bayer T, Aranda M, Daniels C, Shibi A, Chavanich S, Voolstra CR. 2014. Bacterial profiling of white plague disease in a comparative coral species framework. *ISME J* 8:31–39. <https://doi.org/10.1038/ismej.2013.127>.
- Gignoux-Wolfsohn SA, Aronson FM, Vollmer SV. 2017. Complex interactions between potentially pathogenic, opportunistic, and resident bacteria emerge during infection on a reef-building coral. *FEMS Microbiol Ecol* 93:fix080. <https://doi.org/10.1093/femsec/fix080>.
- Mohamed AR, Sweet M. 2019. Current knowledge of coral diseases present within the Red Sea, p 387–400. In *Oceanographic and biological aspects of the Red Sea*. Springer, Cham, Switzerland.
- Thompson FL, Hoste B, Thompson CC, Huys G, Swings J. 2001. The coral bleaching *Vibrio shiloi* Kushmaro et al., 2001 is a later synonym of *Vibrio mediterranei* Pujalte and Garay 1986. *Syst Appl Microbiol* 24:516–519. <https://doi.org/10.1078/0723-2020-00065>.
- Kushmaro A, Rosenberg E, Fine M, Loya Y. 1997. Bleaching of the coral *Oculina patagonica* by *Vibrio* AK-1. *Mar Ecol Prog Ser* 147:159–165. <https://doi.org/10.3354/meps147159>.
- Ben-Haim Y, Zicherman-Keren M, Rosenberg E. 2003. Temperature-regulated bleaching and lysis of the coral *Pocillopora damicornis* by the novel pathogen *Vibrio coralliilyticus*. *Appl Environ Microbiol* 69:4236–4242. <https://doi.org/10.1128/aem.69.7.4236-4242.2003>.
- Sussman M, Willis BL, Victor S, Bourne DG. 2008. Coral pathogens identified for white syndrome (WS) epizootics in the Indo-Pacific. *PLoS One* 3:e2393. <https://doi.org/10.1371/journal.pone.0002393>.
- Arotsker L, Siboni N, Ben-Dov E, Kramarsky-Winter E, Loya Y, Kushmaro A. 2009. *Vibrio* sp. as a potentially important member of the Black Band Disease (BBD) consortium in *Favia* sp. corals. *FEMS Microbiol Ecol* 70:515–524. <https://doi.org/10.1111/j.1574-6941.2009.00770.x>.
- Vidal-Dupiol J, Ladrrière O, Meistertzheim AL, Fouré L, Adjeroud M, Mitta G. 2011. Physiological responses of the scleractinian coral *Pocillopora damicornis* to bacterial stress from *Vibrio coralliilyticus*. *J Exp Biol* 214:1533–1545. <https://doi.org/10.1242/jeb.053165>.
- Mills E, Shechtman K, Loya Y, Rosenberg E. 2013. Bacteria appear to play important roles in both causing and preventing the bleaching of the coral *Oculina patagonica*. *Mar Ecol Prog Ser* 489:155–162. <https://doi.org/10.3354/meps10391>.
- Rubio-Portillo E, Yarza P, Peñalver C, Ramos-Esplá AA, Antón J. 2014. New insights into *Oculina patagonica* coral diseases and their associated *Vibrio* spp. communities. *ISME J* 8:1794–1807. <https://doi.org/10.1038/ismej.2014.33>.

16. Reshef L, Ron E, Rosenberg E. 2008. Genome analysis of the coral bleaching pathogen *Vibrio shiloi*. *Arch Microbiol* 190:185–194. <https://doi.org/10.1007/s00203-008-0388-0>.
17. Santos EDO, Alves N, Dias GM, Mazotto AM, Vermelho A, Vora GJ, Wilson B, Beltran VH, Bourne DG, Le Roux F, Thompson FL. 2011. Genomic and proteomic analyses of the coral pathogen *Vibrio coralliilyticus* reveal a diverse virulence repertoire. *ISME J* 5:147183. <https://doi.org/10.1038/ismej.2011.19>.
18. Kimes NE, Grim CJ, Johnson WR, Hasan NA, Tall BD, Kothary MH, Kiss H, Munk AC, Tapia R, Green L, Dettler C, Bruce DC, Brettin TS, Colwell RR, Morris PJ. 2012. Temperature regulation of virulence factors in the pathogen *Vibrio coralliilyticus*. *ISME J* 6:835–846. <https://doi.org/10.1038/ismej.2011.154>.
19. Vezzulli L, Previati M, Pruzzo C, Marchese A, Bourne DG, Cerrano C, VibrioSea Consortium. 2010. *Vibrio* infections triggering mass mortality events in a warming Mediterranean Sea. *Environ Microbiol* 12: 2007–2019. <https://doi.org/10.1111/j.1462-2920.2010.02209.x>.
20. Ushijima B, Videau P, Poscablo D, Stengel JW, Beurmann S, Burger AH, Aeby GS, Callahan SM. 2016. Mutation of the *toxR* or *mshA* genes from *Vibrio coralliilyticus* strain OCN014 reduces infection of the coral *Acropora cytherea*. *Environ Microbiol* 18:4055–4067. <https://doi.org/10.1111/1462-2920.13428>.
21. Kinnula H, Mappes J, Sundberg LR. 2017. Coinfection outcome in an opportunistic pathogen depends on the inter-strain interactions. *BMC Evol Biol* 17:77. <https://doi.org/10.1186/s12862-017-0922-2>.
22. Medema MH, Blin K, Cimermanic P, de Jager V, Zakrzewski P, Fischbach MA, Weber T, Takano E, Breitling R. 2011. antiSMASH: rapid identification, annotation and analysis of secondary metabolite biosynthesis gene clusters in bacterial and fungal genome sequences. *Nucleic Acids Res* 39:339–346.
23. Harrison F, Paul J, Massey RC, Buckling A. 2008. Interspecific competition and siderophore-mediated cooperation in *Pseudomonas aeruginosa*. *ISME J* 2:49–55. <https://doi.org/10.1038/ismej.2007.96>.
24. Leinweber A, Weigert M, Kümmerli R. 2018. The bacterium *Pseudomonas aeruginosa* senses and gradually responds to interspecific competition for iron. *Evolution* 72:1515–1528. <https://doi.org/10.1111/evo.13491>.
25. Lamont IL, Beare PA, Ochsnor U, Vasil AI, Vasil ML. 2002. Siderophore-mediated signaling regulates virulence factor production in *Pseudomonas aeruginosa*. *Proc Natl Acad Sci U S A* 99:7072–7077. <https://doi.org/10.1073/pnas.092016999>.
26. Banin E, Vasil ML, Greenberg EP. 2005. Iron and *Pseudomonas aeruginosa* biofilm formation. *Proc Natl Acad Sci U S A* 102:11076–11081. <https://doi.org/10.1073/pnas.0504266102>.
27. Burbank L, Mohammadi M, Roper MC. 2015. Siderophore-mediated iron acquisition influences motility and is required for full virulence of the xylem-dwelling bacterial phytopathogen *Pantoea stewartii* subsp. *stewartii*. *Appl Environ Microbiol* 81:139–148. <https://doi.org/10.1128/AEM.02503-14>.
28. Payne SM, Mey AR, Wyckoff EE. 2016. *Vibrio* iron transport: evolutionary adaptation to life in multiple environments. *Microbiol Mol Biol Rev* 80:69–90. <https://doi.org/10.1128/MMBR.00046-15>.
29. Costa TR, Felisberto-Rodrigues C, Meir A, Prevost MS, Redzej A, Trokter M, Waksman G. 2015. Secretion systems in Gram-negative bacteria: structural and mechanistic insights. *Nat Rev Microbiol* 13:343–359. <https://doi.org/10.1038/nrmicro3456>.
30. Basler A, Mekalanos JJ. 2012. Type 6 secretion dynamics within and between bacterial cells. *Science* 337:815–815. <https://doi.org/10.1126/science.1222901>.
31. Joshi A, Kostiuk B, Rogers A, Teschler J, Pukatzki S, Yildiz FH. 2017. Rules of engagement: the type VI secretion system in *Vibrio cholerae*. *Trends Microbiol* 25:267–279. <https://doi.org/10.1016/j.tim.2016.12.003>.
32. Cornforth DM, Foster KR. 2013. Competition sensing: the social side of bacterial stress responses. *Nat Rev Microbiol* 11:285–293. <https://doi.org/10.1038/nrmicro2977>.
33. Darwin AJ, Miller VL. 2001. The *psp* locus of *Yersinia enterocolitica* is required for virulence and for growth in vitro when the *Ysc* type III secretion system is produced. *Mol Microbiol* 39:429–444. <https://doi.org/10.1046/j.1365-2958.2001.02235.x>.
34. Wallrodt I, Jelsbak L, Thomsen LE, Brix L, Lemire S, Gautier L, Nielsen DS, Jovanovic G, Buck M, Olsen JE. 2014. Removal of the phage-shock protein PspB causes reduction of virulence in *Salmonella enterica* serovar Typhimurium independently of NRAMP1. *J Med Microbiol* 63: 788–795. <https://doi.org/10.1099/jmm.0.072223-0>.
35. Burbank LP, Stenger DC. 2016. A temperature-independent cold-shock protein homolog acts as a virulence factor in *Xylella fastidiosa*. *Mol Plant Microbe Interact* 29:335–344. <https://doi.org/10.1094/MPMI-11-15-0260-R>.
36. McCarter LL. 2004. Dual flagellar systems enable motility under different circumstances. *J Mol Microbiol Biotechnol* 7:18–29. <https://doi.org/10.1159/000077866>.
37. Merino S, Shaw JG, Tomas JM. 2006. Bacterial lateral flagella: an inducible flagella system. *FEMS Microbiol Lett* 263:127–135. <https://doi.org/10.1111/j.1574-6968.2006.00403.x>.
38. González Y, Venegas D, Mendoza-Hernandez G, Camarena L, Dreyfus G. 2010. Na⁺- and H⁺-dependent motility in the coral pathogen *Vibrio shilonii*. *FEMS Microbiol Lett* 312:142–150. <https://doi.org/10.1111/j.1574-6968.2010.02110.x>.
39. Tomich M, Planet PJ, Figurski DH. 2007. The *tad* locus: postcards from the widespread colonization island. *Nat Rev Microbiol* 5:363–375. <https://doi.org/10.1038/nrmicro1636>.
40. Watnick PI, Fullner KJ, Kolter R. 1999. A role for the mannose-sensitive hemagglutinin in biofilm formation by *Vibrio cholerae* El Tor. *J Bacteriol* 181:3606–3609. <https://doi.org/10.1128/JB.181.11.3606-3609.1999>.
41. Finlay BB, Falkow S. 1997. Common themes in microbial pathogenicity revisited. *Microbiol Mol Biol Rev* 61:136–169. <https://doi.org/10.1128/61.2.136-169.1997>.
42. Fasano A, Fiorentini C, Donelli G, Uzzau S, Kaper JB, Margaretten K, Ding X, Guandalini S, Comstock L, Goldblum SE. 1995. Zonula occludens toxin modulates tight junctions through protein kinase C-dependent actin reorganization, in vitro. *J Clin Invest* 96:710–720. <https://doi.org/10.1172/JCI118114>.
43. Gottesman S, McCullen CA, Guillier M, Vanderpool CK, Majdalani N, Benhammou J, Thompson KM, FitzGerald PC, Sowa NA, FitzGerald DJ. 2006. Small RNA regulators and the bacterial response to stress. *Cold Spring Harbor Symp Quant Biol* 71:1–11. <https://doi.org/10.1101/sqb.2006.71.016>.
44. Murphy ER, Payne SM. 2007. RyhB, an iron-responsive small RNA molecule, regulates *Shigella dysenteriae* virulence. *Infect Immun* 75: 3470–3477. <https://doi.org/10.1128/AI.00112-07>.
45. Chatterjee A, Cui Y, Liu Y, Dumenyo CK, Chatterjee AK. 1995. Inactivation of *rsmA* leads to overproduction of extracellular pectinases, cellulases, and proteases in *Erwinia carotovora* subsp. *carotovora* in the absence of the starvation/cell density-sensing signal, N-(3-oxohexanoyl)-L-homoserine lactone. *Appl Environ Microbiol* 61:1959–1967. <https://doi.org/10.1128/AEM.61.5.1959-1967.1995>.
46. Wang X, Dubey AK, Suzuki K, Baker CS, Babitzke P, Romeo T. 2005. CsrA post-transcriptionally represses *pgaABCD*, responsible for synthesis of a biofilm polysaccharide adhesin of *Escherichia coli*. *Mol Microbiol* 56: 1648–1663. <https://doi.org/10.1111/j.1365-2958.2005.04648.x>.
47. Cui Y, Chatterjee A, Yang H, Chatterjee AK. 2008. Regulatory network controlling extracellular proteins in *Erwinia carotovora* subsp. *carotovora*: FlhDC, the master regulator of flagellar genes, activates *rsmB* regulatory RNA production by affecting *gacA* and *hexA* (*lrhA*) expression. *J Bacteriol* 190:4610–4623. <https://doi.org/10.1128/JB.01828-07>.
48. Aarons S, Abbas A, Adams C, Fenton A, O’Gara FA. 2000. Regulatory RNA (*PrrB* RNA) modulates expression of secondary metabolite genes in *Pseudomonas fluorescens* F113. *J Bacteriol* 182:3913–3919. <https://doi.org/10.1128/jb.182.14.3913-3919.2000>.
49. Sugijura T, Fukuda T, Miyamoto T, Waku K. 1992. Distribution of alkyl and alkenyl ether-linked phospholipids and platelet-activating factor-like lipid in various species of invertebrates. *BBA-LIPID Lipid Met* 1126: 298–308. [https://doi.org/10.1016/0005-2760\(92\)90244-P](https://doi.org/10.1016/0005-2760(92)90244-P).
50. Garg N, Kapono C, Lim YW, Koyama N, Vermeij MJA, Conrad D, Rohwer F, Dorrestein PC. 2015. Mass spectral similarity for untargeted metabolomics data analysis of complex mixtures. *Int J Mass Spectrom* 377: 719–717. <https://doi.org/10.1016/j.ijms.2014.06.005>.
51. Quinn RA, Vermeij MJA, Hartmann AC, Galtier d’Auriac I, Benler S, Haas A, Quistad SD, Lim YW, Little M, Sandin S, Smith JE, Dorrestein PC, Rohwer F. 2016. Metabolomics of reef benthic interactions reveals a bioactive lipid involved in coral defence. *Proc Biol Sci* 283:20160469. <https://doi.org/10.1098/rspb.2016.0469>.
52. Hartmann AC, Petras D, Quinn RA, Protsyuk I, Archer FI, Ransome E, Williams GJ, Bailey BA, Vermeij MJA, Alexandrov T, Dorrestein PC, Rohwer FL. 2017. Meta-mass shift chemical profiling of metabolomes from coral reefs. *Proc Natl Acad Sci U S A* 114:11685–11690. <https://doi.org/10.1073/pnas.1710248114>.
53. Müller WEG, Klemt M, Thakur NL, Schröder HC, Aiello A, D’Esposito M, Menna M, Fattorusso E. 2004. Molecular/chemical ecology in sponges:

- evidence for an adaptive antibacterial response in *Suberites domuncula*. *Mar Biol* 144:19–29. <https://doi.org/10.1007/s00227-003-1184-7>.
54. Rubio-Portillo E, Santos F, Martínez-García M, de Los Ríos A, Ascaso C, Souza-Egipsy V, Ramos-Esplá AA, Anton J. 2016. Structure and temporal dynamics of the bacterial communities associated to microhabitats of the coral *Oculina patagonica*. *Environ Microbiol* 18:4564–4578. <https://doi.org/10.1111/1462-2920.13548>.
 55. Cervino JM, Thompson FL, Gomez-Gil B, Lorence EA, Goreau TJ, Hayes RL, Winiarski-Cervino KB, Smith GW, Huguen K, Bartels E. 2008. The *Vibrio* core group induces yellow band disease in Caribbean and Indo-Pacific reef-building corals. *J Appl Microbiol* 105:1658–1671. <https://doi.org/10.1111/j.1365-2672.2008.03871.x>.
 56. Luna GM, Bongiorni L, Gili C, Biavasco F, Danovaro R. 2010. *Vibrio harveyi* as a causative agent of the white syndrome in tropical stony corals. *Environ Microbiol Rep* 2:120–127. <https://doi.org/10.1111/j.1758-2229.2009.00114.x>.
 57. Darshanee Ruwandepika HA, Sanjeewa Prasad Jayaweera T, Paban Bhowmick P, Karunasagar I, Bossier P, Defoirdt T. 2012. Pathogenesis, virulence factors and virulence regulation of *Vibrios* belonging to the Harveyi clade. *Rev Aquacult* 4:59–74. <https://doi.org/10.1111/j.1753-5131.2012.01061.x>.
 58. Munoz R, Yarza P, Ludwig W, Euzéby J, Amann R, Schleifer K-H, Glöckner FO, Rosselló-Móra R. 2011. Release LTPs104 of the all-species living tree. *Syst Appl Microbiol* 34:169–170. <https://doi.org/10.1016/j.syapm.2011.03.001>.
 59. Bolger AM, Lohse M, Usadel B. 2014. Trimmomatic: a flexible trimmer for Illumina sequence data. *Bioinformatics* 30:2114–2120. <https://doi.org/10.1093/bioinformatics/btu170>.
 60. Bankevich A, Nurk S, Antipov D, Gurevich AA, Dvorkin M, Kulikov AS, Lesin VM, Nikolenko SI, Pham S, Prjibelski AD, Pyskin AV, Sirotkin AV, Vyahhi N, Tesler G, Alekseyev MA, Pevzner PA. 2012. SPAdes: a new genome assembly algorithm and its applications to single-cell sequencing. *J Comput Biol* 19:455–477. <https://doi.org/10.1089/cmb.2012.0021>.
 61. Hyatt D, Chen GL, LoCascio PF, Land ML, Larimer FW, Hauser LJ. 2010. Prodigal: prokaryotic gene recognition and translation initiation site identification. *BMC Bioinformatics* 11:119. <https://doi.org/10.1186/1471-2105-11-119>.
 62. Bateman A, Coin L, Durbin R, Finn RD, Hollich V, Griffiths-Jones S. 2004. The Pfam protein families database. *Nucleic Acids Res* 32(Database issue):D138–D141. <https://doi.org/10.1093/nar/gkh121>.
 63. Tatusov RL, Natale DA, Garkavtsev IV, Tatusova TA, Shankavaram UT, Rao BS, Kiryutin B, Galperin MY, Fedorova ND, Koonin EV. 2001. The COG database: new developments in phylogenetic classification of proteins from complete genomes. *Nucleic Acids Res* 29:22–28. <https://doi.org/10.1093/nar/29.1.22>.
 64. Haft DH, Loftus BJ, Richardson DL, Yang F, Eisen JA, Paulsen IT, White O. 2001. TIGRFAMs: a protein family resource for the functional identification of proteins. *Nucleic Acids Res* 29:41–43. <https://doi.org/10.1093/nar/29.1.41>.
 65. Le S-Y, Maizel JV, Zhang K. 2004. An algorithm for detecting homologues of known structured RNAs in genomes. *Proc IEEE Comput Syst Bioinform Conf* 2004:300–310. <https://doi.org/10.1109/csb.2004.1332443>.
 66. Goris J, Konstantinidis KT, Klappenbach JA, Coenye T, Vandamme P, Tiedje JM. 2007. DNA-DNA hybridization values and their relationship to whole-genome sequence similarities. *Int J Syst Evol Microbiol* 57:81–91. <https://doi.org/10.1099/ijs.0.64483-0>.
 67. Parks DH, Imelfort M, Skennerton CT, Hugenholtz P, Tyson GW. 2015. CheckM: assessing the quality of microbial genomes recovered from isolates, single cells, and metagenomes. *Genome Res* 25:1043–1055. <https://doi.org/10.1101/gr.186072.114>.
 68. Lowe TM, Chan PP. 2016. tRNAscan-SE On-line: integrating search and context for analysis of transfer RNA genes. *Nucleic Acids Res* 44:W54–W57. <https://doi.org/10.1093/nar/gkw413>.
 69. Carver T, Berriman M, Tivey A, Patel C, Böhme U, Barrell BG, Parkhill J, Rajandream M-A. 2008. Artemis and ACT: viewing, annotating and comparing sequences stored in a relational database. *Bioinformatics* 24:2672–2676. <https://doi.org/10.1093/bioinformatics/btn529>.
 70. Rice P, Longden I, Bleasby A. 2000. EMBOSS: the European molecular biology open software suite. *Trends Genet* 16:276–277. [https://doi.org/10.1016/S0168-9525\(00\)02024-2](https://doi.org/10.1016/S0168-9525(00)02024-2).
 71. Schmieder R, Edwards R. 2011. Quality control and preprocessing of metagenomic datasets. *Bioinformatics* 27:863–864. <https://doi.org/10.1093/bioinformatics/btr026>.
 72. Langmead B, Salzberg SL. 2012. Fast gapped-read alignment with Bowtie 2. *Nat Methods* 9:357–359. <https://doi.org/10.1038/nmeth.1923>.
 73. Anders S, Huber W. 2012. Differential expression of RNA-Seq data at the gene level—the DESeq package. European Molecular Biology Laboratory (EMBL), Heidelberg, Germany.
 74. Cui X, Lu Z, Wang S, Jing-Yan Wang J, Gao X. 2016. CMsearch: simultaneous exploration of protein sequence space and structure space improves not only protein homology detection but also protein structure prediction. *Bioinformatics* 32:i332–i340. <https://doi.org/10.1093/bioinformatics/btw271>.
 75. Griffiths-Jones S, Moxon S, Marshall M, Khanna A, Eddy SR, Bateman A. 2005. Rfam: annotating non-coding RNAs in complete genomes. *Nucleic Acids Res* 33:121–124. <https://doi.org/10.1093/nar/gki081>.
 76. Lagesen K, Hallin P, Rødland EA, Staerfeldt H-H, Rognes T, Ussery DW. 2007. RNAmmer: consistent and rapid annotation of ribosomal RNA genes. *Nucleic Acids Res* 35:3100–3108. <https://doi.org/10.1093/nar/gkm160>.
 77. Jeffrey ST, Humphrey GF. 1975. New spectrophotometric equations for determining chlorophylls a, b, c1 and c2 in higher plants, algae and natural phytoplankton. *Biochem Physiol Pfl* 167:191–194. [https://doi.org/10.1016/S0015-3796\(17\)30778-3](https://doi.org/10.1016/S0015-3796(17)30778-3).
 78. Rodriguez-R LM, Konstantinidis KT. 2016. The enveomics collection: a toolbox for specialized analyses of microbial genomes and metagenomes. *PeerJ Preprints* 4:e1900v1. <https://doi.org/10.7287/peerj.preprints.1900v1>.
 79. Pluskal T, Castillo S, Villar-Briones A, Oresic M. 2010. MZmine 2: modular framework for processing, visualizing, and analyzing mass spectrometry-based molecular profile data. *BMC Bioinformatics* 11:395. <https://doi.org/10.1186/1471-2105-11-395>.
 80. Olivon F, Grelier G, Roussi F, Litaudon M, Touboul D. 2017. MZmine 2 data-preprocessing to enhance molecular networking reliability. *Anal Chem* 89:7836–7840. <https://doi.org/10.1021/acs.analchem.7b01563>.
 81. Watrous J, Roach P, Alexandrov T, Heath BS, Yang JY, Kersten RD, van der Voort M, Pogliano K, Gross H, Raaijmakers JM, Moore BS, Laskin J, Bandeira N, Dorrestein PC. 2012. Mass spectral molecular networking of living microbial colonies. *Proc Natl Acad Sci U S A* 109:1743–1752.
 82. Wang M, Carver JJ, Phelan VV, Sanchez LM, Garg N, Peng Y, Nguyen DD, Watrous J, Kapono CA, Luzzatto-Knaan T, Porto C, Bouslimani A, Melnik AV, Meehan MJ, Liu W-T, Crüsemann M, Boudreau PD, Esquenazi E, Sandoval-Calderón M, Kersten RD, Pace LA, Quinn RA, Duncan KR, Hsu C-C, Floros DJ, Gavilan RG, Kleigrewe K, Northen T, Dutton RJ, Parrot D, Carlson EE, Aigle B, Michelsen CF, Jelsbak L, Sohlenkamp C, Pevzner P, Edlund A, McLean J, Piel J, Murphy BT, Gerwick L, Liaw C-C, Yang Y-L, Humpf H-U, Maansson M, Keyzers RA, Sims AC, Johnson AR, Sidebottom AM, Sedio BE, et al. 2016. Sharing and community curation of mass spectrometry data with global natural products social molecular networking. *Nat Biotechnol* 34:828–837. <https://doi.org/10.1038/nbt.3597>.
 83. Sumner LW, Amberg A, Barrett D, Beale MH, Beger R, Daykin CA, Fan TW-M, Fiehn O, Goodacre R, Griffin JL, Hankemeier T, Hardy N, Harnly J, Higashi R, Kopka J, Lane AN, Lindon JC, Marriott P, Nicholls AW, Reilly MD, Thaden JJ, Viant MR. 2007. Proposed minimum reporting standards for chemical analysis. *Metabolomics* 3:211–221. <https://doi.org/10.1007/s11306-007-0082-2>.
 84. Schymanski EL, Singer HP, Longrée P, Loos M, Ruff M, Stravs MA, Ripollés Vidal C, Hollender J. 2014. Identifying small molecules via high resolution mass spectrometry: communicating confidence. *Environ Sci Technol* 48:1811–1819. <https://doi.org/10.1021/es4044374>.
 85. Chong J, Soufan O, Li C, Caraus I, Li S, Bourque G, Xia J. 2018. MetaboAnalyst 4.0: towards more transparent and integrative metabolomics analysis. *Nucleic Acids Res* 46:486–494. <https://doi.org/10.1093/nar/gky310>.
 86. Chong J, Yamamoto M, Xia J. 2019. MetaboAnalystR 2.0: from raw spectra to biological insights. *Metabolites* 9:57. <https://doi.org/10.3390/metabo9030057>.
 87. Sussman M, Mieog JC, Doyle J, Victor S, Willis BL, Bourne DG. 2009. *Vibrio* zinc-metalloprotease causes photoinactivation of coral endosymbionts and coral tissue lesions. *PLoS One* 4:e4511. <https://doi.org/10.1371/journal.pone.0004511>.